Advanced Mathematical Models & Applications
Vol.6, No.1, 2021, pp.45-58

Jomard Publishing

ANALYSIS OF THE DYNAMICS OF FREIGHT CARS WITH LATERAL DISPLACEMENT OF THE FRONT BOGIE

Angela O. Shvets*

Dnipro National University of Railway Transport named after Academician V. Lazaryan, Department of Theoretical and Structural Mechanics, Dnipro, Ukraine

Abstract. The importance of traffic safety issues increases with train speed increase. The question of determining the permissible speeds, which is associated with the assessment of the dynamic qualities of the rolling stock is especially important. A quantitative assessment of dynamic indicators can be obtained by the method of mathematical modeling. The article is devoted to the study of the influence of lateral displacement of gondola car bogies on their main dynamic and interaction indicators between rolling stock and rails. Theoretical study is conducted using the model of spatial vibrations of coupling of five cars in the freight train. During the calculations the change in the rotation angle of the central axle of the car body was considered, which leads to the mutual transverse displacement of the bogies. The rear bogie of the freight car is located along the longitudinal track axle, and the front bogie has a transverse displacement corresponding to the rotation angle of the body along the track axle in the range from 0 to 0.01 radians with a plus sign, which increases the striking angle of the front wheel set on the outer rail. As a result of the research, the dependencies of the dynamic indicators of a freight car on the value of the body rotation angle and the movement speed were obtained. Based on the theoretical calculations, the influence of the lateral displacement of the car's running gears on the dynamic qualities of the rolling stock and interaction indicators of the rolling stock with the rail track, taking into account the movement speed along a curvilinear track section with irregularities, is assessed.

Keywords: dynamic indicators, bogie displacement, gondola, movement speed.
AMS Subject Classification: 70Q05.
Corresponding author: Angela O. Shvets, Dnipro National University of Railway Transport named after Academician V. Lazaryan, Department of Theoretical and Structural Mechanics, Dnipro, Ukraine,
e-mail: *angela_Shvets@ua.fm*
Received: 03 February 2021; Revised: 26 February 2021; Accepted: 04 March 2021; Published: 19 April 2021.

1 Introduction

Determination of permissible movement speeds, which is directly related to the assessment of the dynamic qualities of rolling stock, is an urgent issue in the operation of railway transport (Kurhan & Kurhan, 2019; Shvets et al., 2015). The interaction process between the rolling stock and the track superstructure is determined by many factors; however, the wheels perceive the greatest horizontal lateral forces from the rails on the curved track sections (Kampczyk, 2020; Zhang et al., 2020). These forces, especially in curves of small and medium radius, can be several times higher than the forces arising during the carriage hunting along the straight track sections. In addition, in curves with a radius of less than 600-800 m, the flanges of some wheels are pressed against the outer rail during their movement almost along the entire length of the curve (Lukhanin et al., 2012; Fomin et al., 2019). The main areas of rail breakage due to defects of contact fatigue origin, the overwhelming number of accidents and train crashes caused by the lack of strength of the track structure and rolling stock, as well as the loss of their stability also

occurs on the curved sections of the railway track (Lukhanin et al., 2012; Shvets et al., 2015).

The main reason for the derailment due to the wheel falling inside the gauge is an unacceptable widening of the track, which occurs due to the displacement of the rails by the wheel flange. In this case, the second wheel falls inside the railway gauge. The probability of such derailment is higher in steep curves with wooden sleepers and rails with low lateral stiffness with typical spike fastening due to the rail tilt with the top (Kovalchuk, et al., 2019; Shvets, 2020; Sysyn et al., 2020). In addition, on the sections with wooden sleepers and typical spike fastening, in comparison with the sections with reinforced concrete sleepers, the derailment is significantly facilitated due to the lift of carriages due to the risk of tilting the rails through the separation of the inner edge of the rail base from the plate. During the movement of the bogie with wheel flanges pressed against the rail head, the inner spikes are being displaced and the elastic tilt of the rail takes place. It is followed by the restoration of the track width after the passage of such a bogie. The greater the lateral force of the wheel flanges on the rail head and the lower the vertical force, the more is the displacement of the inner sheathing spikes (Onat & Kayaalp, 2018; Przybylowicz et al., 2020).

The work (Lysyuk, 2002) describes a series of full-scale experiments on wheel derailment due to the carriage lift, thrust and creeping (displacement) of the track. The experiments were carried out with wooden and reinforced concrete sleepers; crushed stone, asbestos and sand ballast; with hammered in and displaced spikes. The scheme of carrying out the field experiments on wheel derailment is shown in Fig. 1.

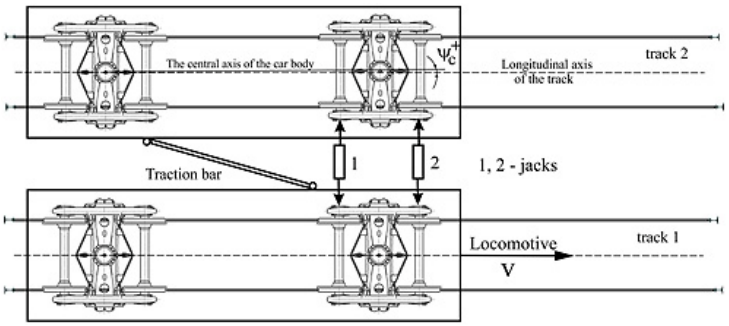

Figure 1: Scheme of full-scale experiments on wheel derailment

Along the first track of the double-track section (Fig. 1) the locomotive moved a 4-axle gondola car loaded with crushed stone up to $P_{st} = 27\ tons/axle$ at a speed of 15-25 km/h. A similar 4-axle gondola car but less loaded was synchronously moved along the second track with the help of a bar. The axle box was fitted with hydraulic thrust jacks 1 and 2, which made it possible to set the thrusting force from 0 to 400 kN (200 kN per axle) in motion. The devices installed along the track recorded displacement of the rail head and base, including its tilt, while simultaneously measuring the forces of lateral horizontal effect of the wheels on the rails with special tensometric wheel sets. The races were repeated many times, in some cases bringing the wheels to the derailment using a thrust or creeping (displacement) of the track. Along the straight track sections on wooden sleepers with a typical spike fastening with fully loaded ($P_{st} < 20\,t/axle$) cars, displacement of the rail base did not exceed 1-1.5 mm with the displacement of the rail head of $5.0 - 6.0mm$.

Increase in the level of interaction forces between the railway carriages and the rail track is also possible in the event of significant wear of wheel sets and rails (Kurhan et al., 2020; Onat & Kayaalp, 2019). The ribs of the center pads and the side edges of the center plates of freight cars wear out during operation and a horizontal backlash is being formed between them, which in some cases exceeds 5 mm. The pivot hole also becomes oval (Muradian et al., 2016a; Muradian et al., 2016b). On the ribs of the center pads in their upper part and on the side edges of the center plates in their lower part, the metal wears out from the action of horizontal forces, the

inner outline of the top of the center pad ribs and the bottom of the center plates are rounded. During operation, the center pivot in freight cars wears out, bends and even breaks, crushing the hole where it is inserted. The eccentricity value in the cross-section of the bogie center pivot can reach more than 10 mm only due to lateral wear of the center pad and center plate (Muradian et al., 2015).

The most common three-piece bogies of 18-100 model have a number of disadvantages, which include the possibility of side frames lozenging under the action of longitudinal components of the friction forces at the contacts of the wheels with the rails, which causes a geometry loss of the bogie frame and the appearance of wheel set axles' misalignment. Design of the pedestal jaw opening of the side frame and the axle-box mount provides for the presence of longitudinal and transverse gaps between the lugs of the axle-box body and the axle-box opening guides, which may also change the nature of their contact. Longitudinal lozenging of side frames relative to each other when driving along curved track sections causes wheel sets turns in the track plane against the direction of the curve. This, in turn, increases the striking angles of the wheel flanges onto the rails, on which their mutual wear depends, since this reduces the contact area of the flange with the side edge of the rail and, accordingly, the specific pressure on it increases, which determines their wear (Shatunov et al., 2020).

In the works (Lukhanin et al., 2012; Shvets, 2020), the transverse displacement of the bogies relative to each other is considered. It is assumed that the rear bogie is located along the longitudinal track axle and the front bogie has a lateral displacement corresponding to the initial rotation angle of the body in the plan relative to the track axle in the range from 0.002 to 0.008 rad with a plus sign, at which the striking angle of the front wheel set increases.

The purpose of this study is to determine the influence of the lateral displacement of a freight car bogie, taking into account the movement speed, on the main dynamic and interaction indicators of rolling stock and the rails in the range from 0 to 0.01 radians, as well as to establish a possible cause of intensive wear of wheels and rails.

2 Methodology

A quantitative assessment of dynamic performance can be obtained by mathematical modeling. A mathematical model describing the spatial vibrations of the car coupling in a train (Fig. 2) was proposed in the work (Danovich & Malysheva, 1998), of which one rail carriage is considered according to the full design scheme ("zero"), and the design schemes of neighboring cars depending on the problem formulation are simplified as the distance from the "zero" carriage increases in both directions.

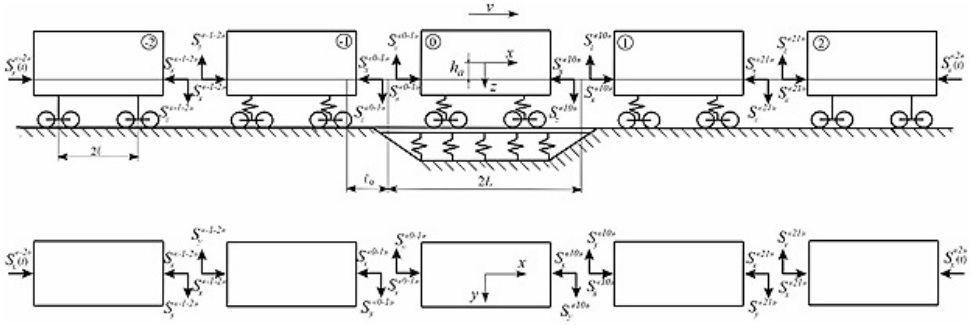

Figure 2: Design scheme of coupling of five freight cars

The longitudinal force acting on the first and the last car of the coupling from the side of the thrown away parts of the train (Fig. 2) at any moment is determined from the solution of the problem of the longitudinal dynamics of the train. Longitudinal forces are considered positive if they cause tension. The forces occurring in the draft gears of the coupling platforms

are determined in accordance with the works (Blokhin & Manashkin, 1982; Shatunov & Shvets, 2020).

Mathematical model of spatial vibrations of a freight car in the form of a multi-mass (body, two bolster beams, four side frames, four wheel sets) nonlinear mechanical system with 58 freedom degrees, which moves along an inertial, elastic-dissipative track (Danovich, 1982) is taken as a design scheme for a "zero" carriage. The cars adjacent to "zero" one are represented by a system with 12 freedom degrees. The last cars of coupling are considered according to an even more simplified scheme – these cars are systems with six degrees of freedom (Danovich & Malysheva, 1998).

Design scheme of a "zero" freight car and positive directions for all movements and rotation angles are shown in Fig. 3.

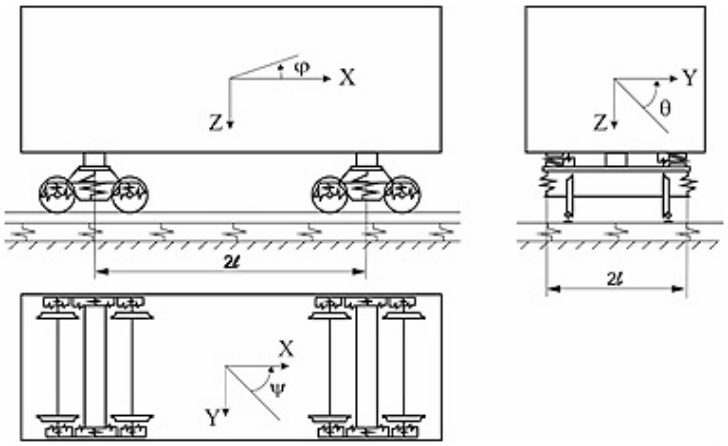

Figure 3: Design scheme of a 4-axle freight car

It is assumed that there are the following connections between the bodies of the system:

- body – bolster: we neglect the gaps between the center plate and the heel, so there are no relative translational movements; the same for pitching of these bodies; hunting and rolling of the bolster beams can occur independently of the corresponding body oscillations;
- bolster – side frame: we assume that there are elastic connections, as a result of which relative translational and angular movements in the horizontal plane (hunting) of these bodies are possible;
- side frame – wheel set: we assume that in this mount there are also connections that allow relative translational and angular movements in the horizontal plane (hunting) of these bodies;
- wheel set – track: connection is assumed to be bidirectional, at the contact point of the wheels with the rails pseudosliding forces arise, which are determined according to Carter's theory, taking into account physical and geometric nonlinearity;
- elastic-viscous and inertial properties of the track base in the vertical and horizontal planes are taken into account only under the "zero" car coupling.

The following nonlinearities are taken into account: forces and force moments of dry friction, body rolling on the heel, impacts after choosing the gaps between the bearings, nonlinear profile of the wheel tread rolling surface, which makes possible taking into account the gap between the flange and the inner edge of the rail head, the nonlinear dependency of the pseudosliding forces on the slippage value and vertical pressure of the wheel on the rail. The following quantities are taken as generalized coordinates for a mechanical system with 58 degrees of freedom:

$q_1 = z,\ q_2 = \varphi,\ q_3 = \theta,\ q_4 = y,\ q_5 = \psi,\ q_n = \theta_i\,(n = 6,7),\ q_n = \psi_i\,(n = 8,9),\ q_n = \psi_{sfij}\,(n = 10 \div 13),\ q_n = y_{sfij}\ (n = 14 \div 17),\ q_n = z_{sfij}\ (n = 18 \div 21),\ q_n = \varphi_{sfij}\ (n = 22 \div 25),\ q_n = \psi_{kim}\ (n = 26 \div 29),\ q_n = y_{kim}\ (n = 30 \div 33),\ q_{\text{n}} = z_{kim}\ (n = 34 \div 37),\ q_n = \theta_{kim}\ (n = 38 \div 41),\ q_n = y_{pimj}\ (n = 42 \div 49),\ q_n = x_{sfij}\ (n = 50 \div 53),\ q_n = x_{kim}\ (n = 54 \div 57),\ q_{58} = x,$ where θ, φ, ψ - rotation angles of the mechanical system relative to the main central axles of inertia; similar movements of the bolster beams are indicated by the index i ($i = 1, 2$- bogie number), side frames – by $sfij$ index ($j = 1$ left, $j = 2$ right side of the car), wheel sets by kim index ($m = 1, 2$ - number of a wheel set in a bogie), rails at the contact points with the wheels (rails movement is provided only in two directions – along the axles Y and Z). The movement of the wheels is indicated by imj index.

For cars with 12 freedom degrees, the following values are taken as generalized coordinates: $q_1^p = z^p,\ q_2^p = \varphi^p,\ q_3^p = \theta^p,\ q_4^p = y^p,\ q_5^p = \psi^p,\ q_{\text{k}}^p = \psi_{\text{i}}^p\ (k = 6,7)\,,\ q_k^p = \psi_{sfi}^p\ (k = 8,9)\,,\ q_k^p = y_{sfi}^p\ (k = 10,11)\,,\ q_{12}^p = x^p$, where $i = 1, 2$ is the bogie number; $p = 1, -1$ is the car number in a coupling.

In the end cars of the coupling, only body oscillations are taken into account: $q_1^p = z^p,\ q_2^p = \varphi^p,\ q_3^p = y^p,\ q_4^p = \theta^p,\ q_5^p = \psi^p,\ q_6^p = x^p$, where $p = 2, -2$ is the car number in a coupling.

In the design schemes describing the oscillations of these cars, the main features of freight car bogies are preserved - side frame lozenging.

The differential equations for the system oscillation are compiled using the Lagrange equation of the second kind:

$$\frac{d}{dt}\left(\frac{\partial T}{\partial \dot{q}_n}\right) - \frac{\partial T}{\partial \dot{q}_n} + \frac{\partial \text{P}}{\partial q_n} + \frac{\partial R}{\partial \dot{q}_n} = Q_n + F_n, \tag{1}$$

where T, P are kinetic and potential energies of the system; R is a system energy dissipation function; q_n are the generalized coordinates; Q_n is the corresponding generalized forces, which are the sum of the interaction forces between the wheel and the rail and the forces acting in the connections between the cars during the train motion; F_n is the external traction or braking forces; n is a number of freedom degrees.

The kinetic and potential energies of the system are determined by the dependencies:

$$T = \frac{1}{2}\sum_{i=1}^{2}\sum_{m=1}^{2}\sum_{j=1}^{2} a_{ni} \cdot \dot{q}_n^2; \tag{2}$$

$$\text{P} = \frac{1}{2}\sum_{i=1}^{2}\sum_{m=1}^{2}\sum_{j=1}^{2} c_{ni} \cdot q_n^2, \tag{3}$$

where a_{ni} are the inertial coefficients; c_{ni} are the stiffness coefficients; q_n are the generalized coordinates. The energy dissipation function of the system is:

$$R = \frac{1}{2}\chi \cdot \sum_{i=1}^{2}\sum_{m=1}^{2}\sum_{j=1}^{2} a_{ni} \cdot \dot{q}_n^2; \tag{4}$$

where χ is an energy dissipation coefficient.

Based on the mathematical model of the coupling movement, a package of applied programs has been developed. The system of differential equations has dynamic connections between coordinates and is reduced to the Cauchy normal form. A combined method is used to integrate the motion equations of freight car coupling in a train. The beginning of the solution (acceleration) was carried out using the Runge-Kutta method, and the continuation using the iterative Adams-Bashforth method.

This paper investigates the influence on the main dynamic and interaction indicators of the rolling stock with the rails of freight cars in the curves of one of the factors, namely, the change in the rotation angle of the central axle of the car body ψ_{c}. The choice of this factor as a research

subject is due to the fact that it depends on the value of the total free transverse acceleration of the car body frame relative to the track axle, including the transverse gap in the track. In turn, the relative elastic and inelastic wheel sliding relative to the rails and the value of the corresponding forces, as well as the geometric conditions of contact between the wheels and the rails depend on the gap in the rail track.

Total free transverse acceleration of the car body frame relative to the track axle in the guiding section along the center pivot (due to the transverse accelerations of the wheel sets in the rail track, the bogie frame relative to the wheel sets, the bolster relative to the frame (bogie) and the body bolster relative to the bolster) is recommended by the regulatory documentation to be considered for four-axle freight cars with bolsterless suspension of bogies $2\delta_0 = 50$mm. Taking into account the fact that the lateral wear of the center pad and center plate can exceed 10 mm, and the inaccuracy of the coupler support location on the end beam of some cars can reach 20 mm, the rotation angle of the central axle of the car body in the calculations was considered to be $\psi_{\text{A}} = 0.01$ rad.

Changing the rotation angle of the central axle of the car body ψ_{A}leads to a lateral bogie displacement relative to each other (Lukhanin et al., 2012; Shvets, 2020). In this case, the rear bogie of the freight car is located along the longitudinal track axle, and the front bogie has a transverse displacement, which corresponds to the body rotation angle in the plan relative to the track axle in the range from 0 to 0.01 rad with a plus sign (Fig. 4), at which the striking angle of the front wheel set onto the outer rail increases.

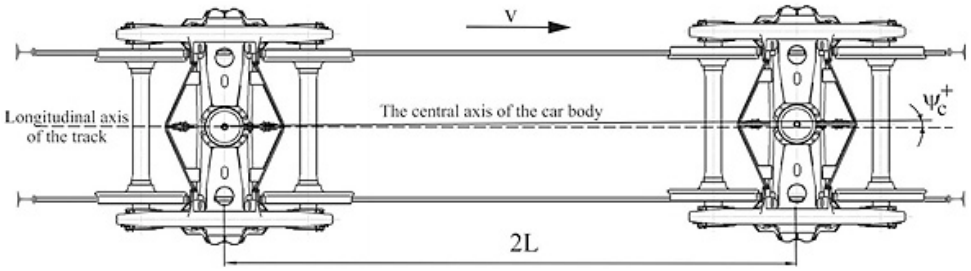

Figure 4: Arrangement of freight car bogies in a rail track

The correspondence of the values between the total free transverse acceleration of the car body frame $2\delta_0$ and the rotation angle of the central axle of the car body are given in Table 1.

Table 1: Correspondence of the values of the parameters under study

Parameter	Correspondence between values					
$2\delta_0$, mm	0	17	35	52	69	87
ψ_{A}, rad	0	0.002	0.004	0.006	0.008	0.010

The study was carried out using a model of spatial vibrations of the coupling of five cars in the train in the right curve, respectively, the left wheel of the first wheel set is climbing on the outer rail. Initial data for the study: movement of a gondola car model 12-532 with typical three-piece bogies 18-100 at speeds in the range of $50 \div 90$km/h in a curve with a radius of 600 m with superelevation of 120 mm. Rails – R65, sleepers – wooden, ballast – crushed stone. The stationary mode of movement was investigated in order to establish the influence of only the factor under consideration. The running gear of the car, the wheel thread and the rail head profile were provided in a normal technical condition.

The grade levels and permissible values of the dynamic quality indicators of freight rolling stock in accordance with the regulatory documentation are given in Table 2.

Table 2: Grade levels and permissible values of the dynamic quality indicators

Indicator	Grade level	Permissible values	
		empty	loaded
Maximum coefficient of dynamic addition of sprung parts (vertical dynamics coefficient of the central suspension stage) $K^{\mathrm{s}}_{\mathrm{dv}}$	excellent	0.5	0.2
	good	0.6	0.35
	satisfactory	0.7	0.4
	permissible	0.75	0.65
Maximum coefficient of dynamic addition of unsprung parts (vertical dynamics coefficient of the axle box suspension stage) $K^{\mathrm{us}}_{\mathrm{dv}}$	excellent	0.6	0.5
	good	0.75	0.7
	satisfactory	0.85	0.8
	permissible	0.98	0.9
Maximum ratio of frame force to static axle loading (horizontal dynamic coefficient) K_{dh}	excellent	0.25	0.2
	good	0.3	0.25
	satisfactory	0.38	0.3
	permissible	0.4	0.38
Derailment stability coefficient K_{ds}	permissible	1.3	

3 Results

To study the dynamic forces and processes acting in the components of the bogie or car body, the maximum coefficients of the dynamic addition of sprung K^s_{dv} and unsprung parts K^{us}_{dv}, the maximum ratio of the frame force to the static axle loading and the derailment stability coefficient K_{ds} are used. Graphs of changes in dynamic indicators when driving along a curved track section $R = 600$ m are shown in Fig. 5, 6.

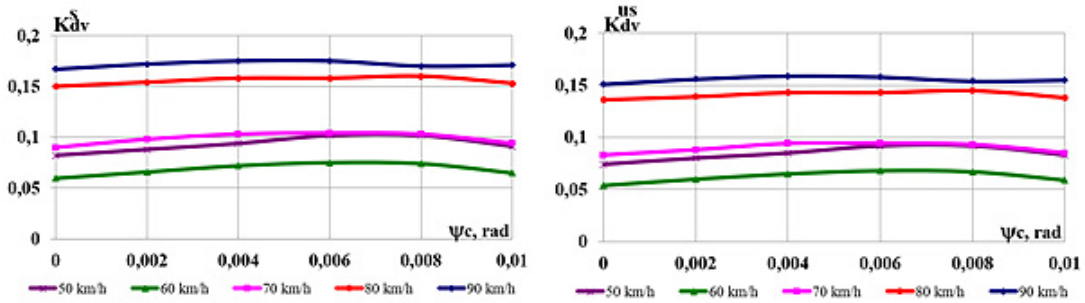

(a) (b)

Figure 5: Graphs of changes in dynamic indicators on the movement speed: (a) coefficient of dynamic addition of sprung parts; (b) coefficient of dynamic addition of unsprung parts

As one can see from Fig. 5, with increase of the body rotation angle in the plan relative to the track axle, the investigated dynamic coefficients generally remain unchanged. In the entire speed range K^s_{dv}, the indicators (Fig. 5,a) and K^{us}_{dv} (Fig. 5,b) in the case of increase ψ_c from 0 to 0.01 rad do not exceed the permissible norm. The grade level is excellent (Table 2).

From the results obtained, it can be concluded that the body rotation angle in the plan relative to the track axle ψ_c in the case of increase in the movement speed does not cause a significant increase in the vertical dynamics indicators in the axlebox and central suspension stages, and their values do not exceed the values determined by the regulatory documentation.

The maximum ratio of the frame force to the static axle loading K_{dh} (Fig. 6,a) and the derailment stability coefficient K_{ds} (Fig. 6,b), in case of increase ψ_c, do not exceed the permissible norm. The grade level for K_{dh} is excellent, for K_{ds} is above the minimum permissible (Table 2).

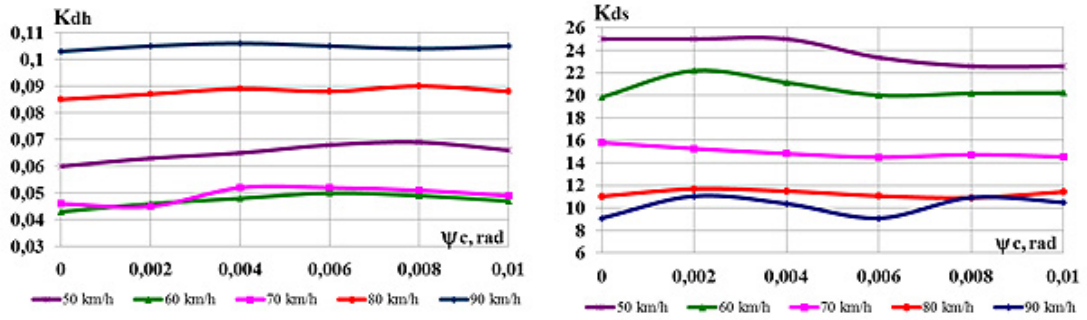

(a) (b)

Figure 6: Graphs of changes in dynamic indicators on the movement speed: (a) maximum ratio of frame force to static axle loading; (b) derailment stability coefficient

Fig. 7 shows the influence of speed on the interaction indicators of the rolling stock with the rails in the curve $R = 600$ m, the lateral force acting on the wheel Y_s from the track and the edge stress in the rail base σ_r. Lateral forces acting from the track on the wheel (horizontal forces) Y_s (Fig. 7,a) increase and have a maximum at $\psi_A = 0.006$ rad and, in comparison with the permissible value of $[Y_s] = 90kN$, to ensure the stability condition against striking of the wheel flanges against the rails, do not have exceedances.

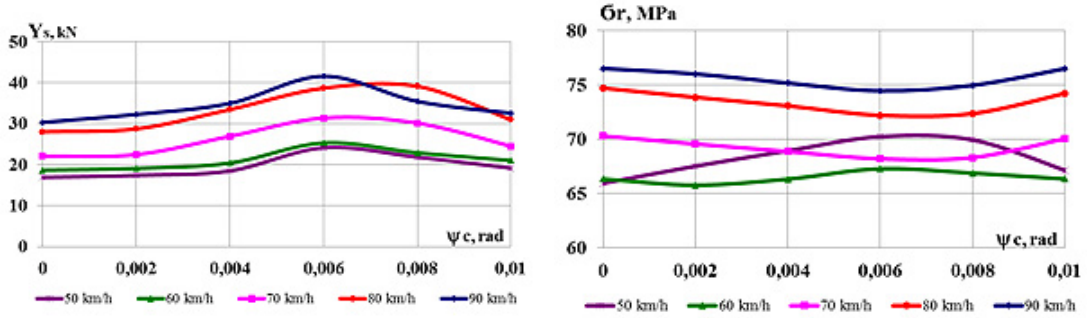

(a) (b)

Figure 7: Graphs of changes in dynamic indicators on the movement speed: (a) lateral force acting from the track on the wheel; (b) edge stress in the rail base

The rotation angle of the central axle of the car body ψ_c largely depends on the interaction forces of the contacting bodies and their relative displacements (relative slip). These forces and displacements are determined by the interaction conditions between the wheels of the rolling stock and the track. Interaction conditions for the bodies of this system depend on both the design, technical condition and modes of movement of the rolling stock, and on the design, condition and parameters of the rail track. But, it is at $2\delta_0 = 52mm$ ($\psi_c = 0.006\,rad$, Table 1) that the maximum values of the lateral force Y_s are obtained. Compared to $\psi_c = 0.005\,rad$, these values are higher by an average of 9.5%.

With an increase in train movement speeds, the dynamic effect on the track of the rolling stock increases and, as a result, stresses in the rail base edges increase. The maximum stresses arising in the edges of the rail base are used as a criterion for establishing the permissible speeds and should not exceed 200 MPa. But in the case of the considered arrangement scheme of freight car bogies in a rail track, a redistribution of vertical and horizontal reactions occurs in

the contact area between the wheel and the rail. According to the results of calculations, the edge stresses (Fig. 7, b) increase with an increase in the movement speed, but they have a minimum precisely at $\psi_c = 0.006\,rad$ in the speed range of $70 \div 90\ km/h$ and a maximum at $50 \div 60\ km/h$. However, the results obtained do not exceed the permissible values for both types of rails – before and after passing the standard tonnage for the track with non-heat-treated R65 rails.

Fig. 8 shows the coefficients of the vertical K_{vdt} and horizontal dynamics K_{vdt} of the track according to the interaction forces of the wheels and the rails.

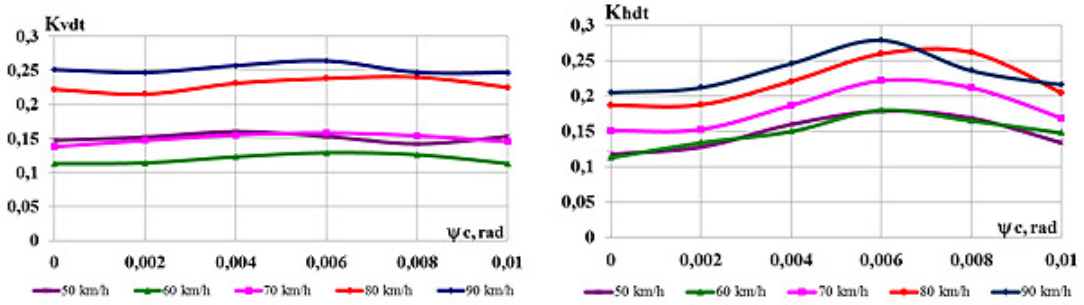

(a) (b)

Figure 8: Graphs of changes in dynamic indicators by the interaction forces of wheels and rails on the speed of movement: (a) vertical dynamics coefficient of the track; (b) horizontal dynamics coefficient of the track

The permissible value of the vertical dynamics coefficient of the track K_{vdt} is calculated in accordance with the permissible dynamic linear loading on the railway track on the group of bogie axles $168kN/m$, for the selected type of rolling stock it is $[K_{vdt}] = 0.45$. The vertical dynamics coefficient of the track K_{vdt} (Fig. 8,a) does not exceed the permissible value.

The horizontal dynamics coefficient of the track K_{hdt} (Fig. 8,b), which is considered a safety criterion against creeping (displacement) of the track panel, does not exceed the permissible value $[K_{hdt}] = 0.4$ and has a significant maximum in the entire range of the considered speeds at $\psi_{\text{A}} = 0.006\,rad$.

Fig. 9 shows the stability coefficients of the e track panel against creeping (displacement) ε and the wear factor of the side edge of the wheel tread F_w.

The permissible value of the stability coefficient of the track panel against the action of lateral forces is $[\varepsilon] = 0.85$. According to the calculation results, the value of stability coefficient of the track panel from the action of lateral forces ε (Fig. 9,a) in the track with crushed stone ballast is $0.3 - 0.56$, which is less than the permissible value.

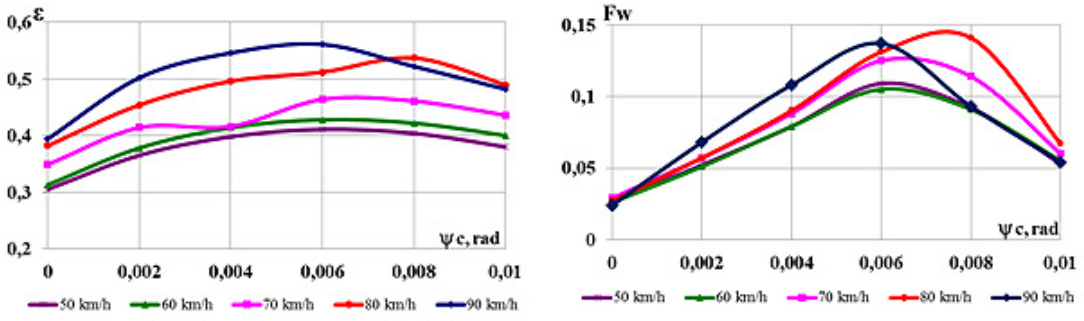

(a) (b)

Figure 9: Graphs of changes in indicators from the movement speed: (a) stability coefficient of the track panel from the action of lateral forces; (b) wear factor of the side edge of the wheel tread

With an increase in the movement speed, for example, at speeds of $70 \div 90$ km/h, the wear factor of the side edge of the wheel tread F_w increases significantly (Fig. 9, b), the corresponding values at $50 \div 60$ km/h are exceeded by an average of 22.43%. As $2\delta_0$ increases from 52 to 87 mm, the flange wear rate decreases, which indicates an increase in the operational life of the wheel set. As one can see from Fig. 9 indicators ε and F_{w} also have maximums at $\psi_c = 0.006$ rad except for a speed of 90 km/h. In this case, the extremes of the considered indicators are shifted by 0.008 rad.

The wear factor of the side edge of the wheel tread F_w is defined as a characteristic equal to the product of the guiding force Y_g acting on the wheel from the side of the track by the angle of hunting (striking) ψ_{ws} of the wheel onto the rail. The influence of the movement speed on these indicators is shown in Fig. 10.

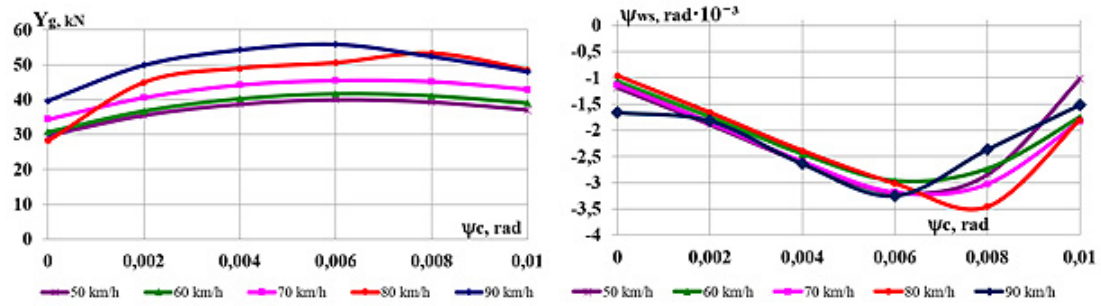

(a) (b)

Figure 10: Graphs of changes in dynamic indicators on the movement speed: (a) guiding force acting from the side of the track on the wheel; (b) hunting of the first wheel set of the front bogie

The guiding forces acting from the side of the track on the wheel Y_g (Fig. 10, a) with increase in the movement speed significantly increase from a speed of 70 km/h. The calculation results show (Fig. 10, b) that the hunting angles of the wheel set ψ_{ws} have maximums at $\psi_c = 0.006$ rad, except for the speed of 80 km/h. In addition, the hunting angles ψ_{ws} have a minus sign, that is, the wheel sets rotate in the track plane against the curve direction in accordance with the accepted rule of signs (Fig. 3).

Let us analyze the hunting of the front ψ_{bg1} (Fig. 11,a) and rear ψ_{bg2} (Fig. 11,b) bogies along the path of the car.

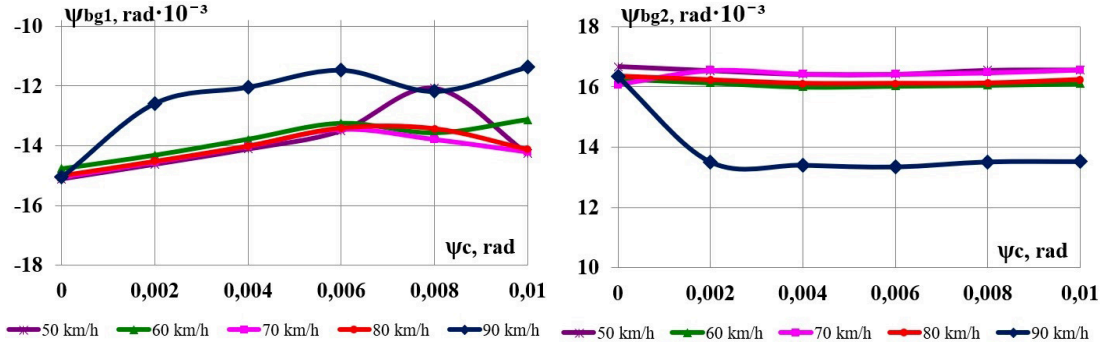

(a) (b)

Figure 11: Graphs of changes in dynamic indicators on the movement speed: (a) hunting of the front bogie; (b) hunting of the rear bogie

Hunting of the front and rear bogies is opposite in direction and ψ_{bg2} exceeds the values ψ_{bg1} for the front bogie. The nature of hunting of the front bogie (Fig. 11, a) differs significantly from the process of hunting of its first wheel set (Fig. 10, b). The process of hunting the rear

bogie ψ_{bg2} along the path at 90 km/h and $\psi_c = 0.002 \div 0.01$ has significantly lower values (Fig. 11, b).

Let us consider the lozenging of the side frames of the front bogie (Fig. 12, a) and the mutual longitudinal movement of the side frame and the axle box of the front wheel set (Fig. 12, b).

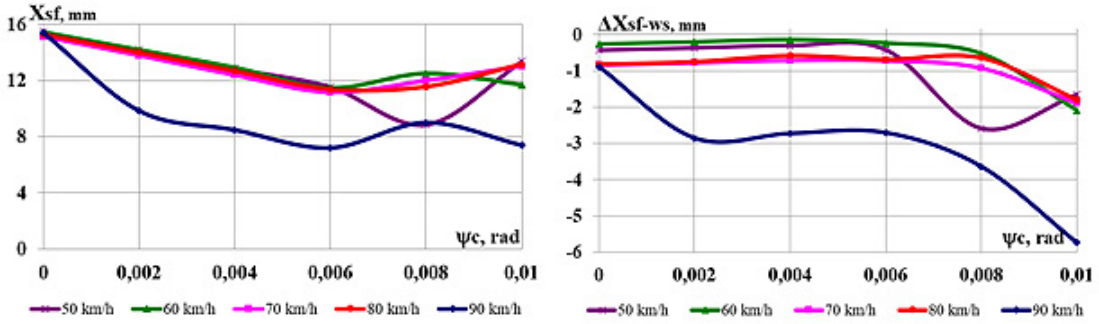

(a) (b)

Figure 12: Graphs of changes in dynamic indicators on the movement speed: (a) lozenging of the side frames of the front bogie; (b) mutual longitudinal movement of the side frame and the axle box of the front wheel set

The results of theoretical studies show that lozenging of side frames of the front bogie X_{sf} (Fig. 12, a) and mutual longitudinal movement of side frame and axle box of the front wheel set ΔE_{sf-ws} (Fig. 12, b) in case of transverse displacement of the bogies relative to each other have insignificant influence on the wear factor of the side edge of the wheel tread F_w. In addition, lozenging of side frames of the front bogie X_{sf} (Fig. 12, a) at $\psi_c = 0.006$ rad have the smallest values in the entire investigated range of speeds.

To establish a possible reason for the intensive wear of wheels and rails, further more detailed study of the interaction process of freight car body with a three-piece bogie is needed when the rotation angle of the central axle of the car body changes.

Since on the sections with wooden sleepers, derailment is significantly facilitated through the carriage lift due to the risk of tilting the rail through the separation of the inner edge of the rail base from the plate and displacement of the inner sheathing spikes, Fig. 13 shows displacement of the rail base y_t and the rail head y_{et}. The higher the movement speed, the more the displacement value y_t of the inner sheathing spikes (Fig. 13, a). In the range of speeds of $50 \div 60 km/h$, the increase in rail base displacement is on average 9.59% for every 10 km/h, and at speeds of $70 \div 90 km/h$, the corresponding values increase on average by 21.1%.

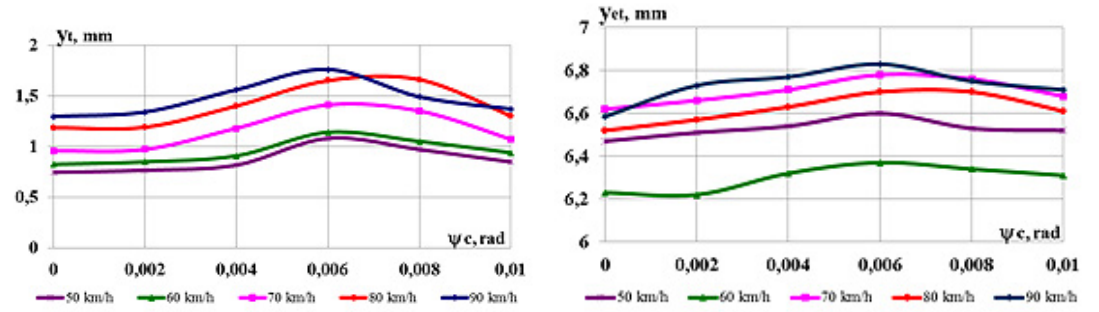

(a) (b)

Figure 13: Graphs of the change in the displacement indicators on the movement speed: (a) rail base; (b) rail head

According to the results of calculations, for displacements of the rail head y_{et} (Fig. 13, b)

there is no such a clear dependency, but both indicators have maximum values at the rotation angle of the central axle of the car body $\psi_c = 0.006$ rad.

The calculations presented in this study were carried out with an axle loading of a car of 21.4 tons per axle and in the range of speeds from $50 \div 90 km/h$ in a curve with a radius of 600 m. Comparison of the calculated results shows satisfactory agreement with experimental data on the values of y_t and y_{et}.

4 Conclusions

The article presents an analysis of the theoretical studies of the main dynamic and interaction indicators of rolling stock and rails on the example of gondola cars. The calculations were performed using a package of applied programs. Based on the theoretical study, the following conclusions can be drawn:

- Maximum coefficients of dynamic addition of sprung K^s_{dv} and unsprung parts K^{us}_{dv}, maximum ratio of the frame force to static axle loading K_{dh}, derailment stability coefficient K_{ds} depend much more on the movement speed than on the rotation angle of the central axle of the car body ψ_c.

- Analyzed interaction indicators of rolling stock with the track do not exceed the standard values and have extremes at $\psi_c = 0.006$ rad.

- A simultaneous increase in the rotation angle of the central axle of the car body ψ_A and the movement speed leads to an increase in the wear factor of wheels and rails.

- With increase in the movement speed by a large value, the inner sheathing spikes y_t and rail heads y_{et} are displaced, both indicators have their maximum values at the rotation angle of the central axle of the car body $\psi_c = 0.006$ rad.

- Comparison of the obtained calculation results shows satisfactory agreement with the experimental data on the values of displacement of the rail base y_t and rail head y_{et}.

References

Blokhin, Ye.P., Manashkin, L.A. (1982). *Train dynamics (unsteady longitudinal oscillations)*: monograph. Publisher Transport, Moscow (in Russian).

Danovich, V.D. (1982). *Spatial cars oscillations in inertia track*. (Thesis of doctor of technical sciences). Dnipropetrovsk National University of Railway Transport named after Academician V. Lazaryan, Dnipropetrovsk. (in Russian).

Danovich, V.D., Malysheva, A.A. (1998). Mathematical model of spatial oscillations of the coupling of five cars moving along a rectilinear section of the track. *Transport. Stress Loading and Durability of a Rolling Stock*, 62-69. (in Russian).

Fomin, O., Shvets, A., Hauser, V., Prokopenko, P. (2019). Transversal displacement of freight wagons bogies. *AIP Conference Proceedings 2198 020002*.

Kampczyk, A. (2020). Measurement of the geometric center of a turnout for the safety of railway infrastructure using MMS and Total Station. *Sensors*, *20*(16), 1-35. doi: https://doi.org/10.3390/s20164467.

Kovalchuk, V., Sysyn, M., Gerber, U., Nabochenko, O., Zarour, J., Dehne, S. (2019). Experimental investigation of the influence of train velocity and travel direction on the dynamic behavior of stiff common crossings. *Facta Univesitatis Series Mechanical Engineering*, *17*(3), 345-356. doi.org/10.22190/FUME190514042K.

Kurhan, M., Kurhan, D., Novik, R., Baydak, S., Hmelevska, N. (2020). Improvement of the railway track efficiency by minimizing the rail wear in curves. *IOP Conference Series: Materials Science and Engineering, Volume 985, 15th International Scientific and Technical Conference "Problems of the railway transport mechanics"* (PRTM 2020) 27-29 May 2020, Dnipro, Ukraine, 985 012001. doi:10.1088/1757-899X/985/1/012001.

Kurhan, M.B., Kurhan, D.M. (2019). Providing the railway transit traffic Ukraine–European Union. *Pollack Periodica*, *14*(2), 27-38. doi: 10.1556/606.2019.14.2.3.

Lukhanin, N.I., Myamlin, S.V., Neduzhaya, L.A., Shvets, A.A. (2012). Freight cars dynamics taking into account transversal displacement of the bogies. *Proc. of the Donetsk Railway Transport Institute*, *29*, 234-241. (in Russian).

Lysyuk, V.S. (2002). *The causes and mechanisms of the vanishing wheel from the rail. The problem of wear of wheels and rails.* Publisher Transport, Moscow, 215 (in Russian).

Muradian, L.A., Shaposhnyk, V.Yu., Mischenko, A.A. (2016). Methodological fundamentals of determination of unpowered rolling stock maintenance characteristics. *Science and Transport Progress*, *1*(61), 169-179. doi: 10.15802/stp2016/61044. (in Russian).

Muradian, L.A., Shaposhnyk, V.Yu., Podosenov, D.O. (2016). Improving the reliability of freight wagons with the use of new manufacturing technologies and regeneration of working surfaces. *Electromagnetic compatibility and safety in railway transport*, *11*, 49-54. doi: 10.15802/ecsrt2016/91337. (in Russian).

Muradyan, L.A., Shaposhnik, V.Yu., Vinstrot, B.U., Mukovoz, S.P. (2015). Tests of promising brake pads on the railways of Ukraine. *Lokomotiv-inform*, *7-8*. 20-22 (in Russian).

Onat, A., Kayaalp, B. (2018). Normal load estimation by using a swarm intelligence based multiple models approach. *4th International Symposium on Railway Systems Engineering (ISERSE'18)*, October 10-12, 2018, Karabuk, Turkey.

Onat, A., Kayaalp, B. (2019). A novel methodology for dynamic weigh in motion system for railway vehicles with traction. *IEEE Transactions on Vehicular Technology*. doi: 10.1109/TVT.2019.2940011.

Przybylowicz, M., Sysyn, M., Parneta, B., Kovalchuk, V., Nabochenko, O. (2020). Experimental and theoretical evaluation of side tamping method for ballasted railway track maintenance. *Transport Problems*, *15*(3), 93-106. 10.21307/tp-2020-036.

Shatunov, O.V., Shvets, A.O., Kirilchuk, O.A., Shvets, A.O. (2019). Research of wheel-rail wear due to non-symmetrical loading of a flat car. *Science and Transport Progress, 4*(82), 102-117. doi: https://doi.org/10.15802/stp2019/177457

Shatunov, O.V., Shvets, A.?. (2020). Flat cars coupling dynamics when transporting long cargo. *Science and Transport Progress, 4*(88), 114-131. doi: https://doi.org/10.15802/stp2020/213381. (in Ukrainian).

Shvets, A.A., Zhelieznov, K.I., Akulov, A.S., Zabolotnyi, A.N., Chabaniuk, Ye.V. (2015). Some aspects of the definition of empty cars stability from squeezing their longitudinal forces in the freight train. *Science and Transport Progress*, *4*(58), 175-189. doi: 10.15802/stp2015/49281. (in Russian).

Shvets, A.O. (2020). Influence on the dynamics of freight cars transverse displacement of bogies. *Science and Transport Progress*, *6*(89), 151-166. doi: 10.15802/stp2019/61045 (in Ukrainian).

Sysyn M., Nabochenko O., Kovalchuk V. (2020). Experimental investigation of the dynamic behavior of railway track with sleeper voids. *Railway Engineering Science*. doi: https://doi.org/10.1007/s40534-020-00217-8.

Zhang, D., Tang, Y., Sun, Z., Peng, Q. (2020). Optimising the location of wagon gravity centre to improve the curving performance. *Vehicle System Dynamics,* 1-15. doi: 10.1080/00423114.2020.1865546.